

# Quasar spectra and the K correction

Lutz Wisotzki

Hamburger Sternwarte, Gojenbergsweg 112, 21029 Hamburg, Germany (lwisotzki@hs.uni-hamburg.de)

Received 9 April 1999 / Accepted 5 November 1999

**Abstract.** A new determination of the optical  $K(z)$  relation for QSOs is presented, derived from multiwavelength photometry of 25 low-redshift QSOs. The relation deviates strongly from the simple picture of single power law spectra as an overall description, but also from previous empirical determinations based on composite spectra. The deviations are particularly significant at low redshifts where  $K(z)$  drops steeply, bending over towards a flatter slope around  $z \approx 0.6$ . The shape of  $K(z)$  does not show any discernible dependency on either QSO luminosity or radio power. There is evidence that the derived relation might also be representative for QSOs at higher redshift up to  $z \simeq 2$ . Under that hypothesis, the resulting rest-frame absolute magnitudes of QSOs are systematically fainter than usually estimated up to now. The inferred global evolution of the optical luminosity function of quasars is substantially reduced. This modification may reconcile the hitherto discrepant evolution rates of optical and X-ray luminosity functions.

**Key words:** galaxies: quasars: general – galaxies: Seyfert – galaxies: evolution – cosmology: observations

## 1. Introduction

The estimation of rest frame luminosities for sources at cosmological distances requires knowledge about the intrinsic spectral shape of each source is required. In optical astronomy, this knowledge is usually represented by a function  $K(z)$  giving the correction to be applied to broad-band photometric measurements expressed in magnitudes. The distance modulus is written as

$$M - m = 5 - 5 \log d_L(z) + A + K(z)$$

where  $A$  quantifies foreground extinction, and  $d_L(z)$  is the luminosity distance. By convention, the  $K$  correction contains also the  $(1+z)$  bandwidth term.

The  $K$  correction for quasars was long assumed to be easily available (compared to the complicated  $K$  terms for galaxies), since QSO spectra seemed to be well-approximated by simple power laws, conveniently parameterised through their ‘spectral index’  $\alpha$  (e.g., Richstone & Schmidt 1980;  $f_\nu \propto \nu^\alpha$ ). Meanwhile, UV spectrophotometry of many Seyfert 1 galaxies and nearby quasars has shown that there are considerable departures

from this simple picture, and that ‘big’ and ‘little blue bumps’ are ubiquitous in basically all these objects, albeit with varying strength. (cf. Elvis et al. 1994)

Nevertheless, quasar spectra are still often treated as ‘power laws’ in luminosity function work. The  $K$  correction is then particularly simple and can be written as  $K(z) = -2.5(\alpha + 1) \log(1+z)$ . Mean spectral indices between  $\alpha \simeq -0.7$  and  $-0.3$  have been suggested, with  $\alpha = -0.5$  being the canonical value (cf. Schmidt & Green 1983; Boyle et al. 1988). The empirical determination of  $K(z)$  published by Cristiani & Vio (1990) includes the features of observed quasar spectra, but on the whole it shows relatively little departure from an  $\alpha = -0.5$  power law relation.

In the following I discuss a novel approach to determine the optical  $K$  correction for quasars, based on multi-wavelength (optical/UV) observations of low-redshift QSOs. This has the advantage that a full array of  $K(z)$  values can be computed for each object in the sample, and the resultant average relation is therefore largely free from evolutionary trends within the sample. The consequences of using this new empirical  $K$  correction for the field of quasar evolution studies are discussed. This analysis will be concentrated on the  $B$  band as it is most commonly used in QSO evolution studies.

## 2. The K correction for quasars

### 2.1. Continuum

The main body of data was taken from the atlas of quasar energy distributions published by Elvis et al. (1994). Of the 47 quasars belonging to that sample, 23 have reasonably complete and well-sampled optical/UV spectrophotometry to be used for an estimation of  $K(z)$  up to  $z = 2.2$  without extrapolations. These objects are at relatively low redshifts ( $z < 0.8$  for all), but all 23 have  $z > 0.08$  and  $M_V < -23$  and are therefore located in the classical quasar domain. The sample is summarised in Table 1.

Two entries have been added: HE 1029–1401, the most luminous  $z < 0.1$  QSO known, was observed quasi-simultaneously in the optical and in the UV by Wisotzki et al. (1991), and these high-quality data are included here. The second addition is the ultraluminous low-redshift object KUV 1821+643, for which quasi-simultaneous optical/UV continuum data were published by Kolman et al. (1993).

**Table 1.** Sample of QSOs used to determine the  $K$  correction. All entries are taken from the collation of Elvis et al. (1994), except HE 1029–1401 (from Wisotzki et al. 1991) and KUV 1821+643 (from Kolman et al. 1993). Absolute magnitudes were measured in the QSO rest frames, for  $H_0 = 50 \text{ km s}^{-1} \text{ Mpc}^{-1}$ ,  $q_0 = 0.5$ . The last column states whether a QSO is radio-loud (RL) or radio-quiet (RQ).

Name	$M_V$	$z$	Radio
PHL 658	−26.4	0.450	RL
PG 0007+106	−23.9	0.089	RL
PG 0026+129	−24.5	0.142	RQ
PG 0052+251	−24.5	0.155	RQ
3C 48	−25.9	0.367	RL
NAB 0205+024	−24.3	0.155	RQ
3C 110	−27.1	0.781	RL
PG 0804+761	−24.3	0.100	RQ
B2 1028+313	−24.0	0.177	RL
HE 1029–1401	−25.0	0.085	RQ
3C 249.1	−25.5	0.311	RL
PG 1116+215	−25.4	0.177	RQ
3C 263	−26.9	0.652	RL
GQ Com	−23.7	0.165	RQ
PG 1211+143	−24.4	0.085	RQ
3C 273	−27.0	0.158	RL
PG 1307+085	−24.6	0.155	RQ
PG 1352+183	−24.1	0.152	RQ
PG 1407+265	−27.7	0.940	RQ
PG 1416–129	−23.5	0.129	RQ
PG 1426+015	−23.9	0.086	RQ
PG 1613+658	−24.2	0.129	RQ
Kaz 102	−23.8	0.136	RQ
KUV 1821+643	−27.1	0.297	RQ
PKS 2128–123	−26.5	0.501	RQ

The data used to compute the  $K$  corrections consist of measurements of the continuum flux in narrow bands centred on regions in the spectra that are free of emission lines. The flux values were interpolated by cubic splines, and the interpolated spectra were then successively redshifted in steps of  $\Delta z = 0.02$ . Artificial broad-band  $B$  magnitudes were computed for each  $z$ , and the values of  $K = B(z) - B(z = 0) + 2.5 \log(1 + z)$  were tabulated as a function of  $z$ . The resulting relations  $K(z)$  for all of the 25 quasars are shown in Fig. 1.

A natural high-redshift limit is  $z = 2.2$  where the  $\text{Ly}\alpha$  emission line enters the  $B$  band. At higher  $z$ , the variable strength of  $\text{Ly}\alpha$  and the effects of Lyman forest absorption create large additional uncertainties in the  $K$  correction; using low-redshift quasars makes little sense in this domain (neither does a power law). Note that the same redshift cutoff is commonly taken as completeness limit of quasar samples based on ultraviolet excess selection criteria.

A mean  $K$  correction relation was then computed by averaging over all  $K$  values at a given  $z$ . This is equivalent to taking the *geometric mean* of the contributing continua, an approach that avoids the bias occurring in the usual construction of composite spectra: The *average* of two spectra with different power-law slopes is not a power-law type spectrum but assumes

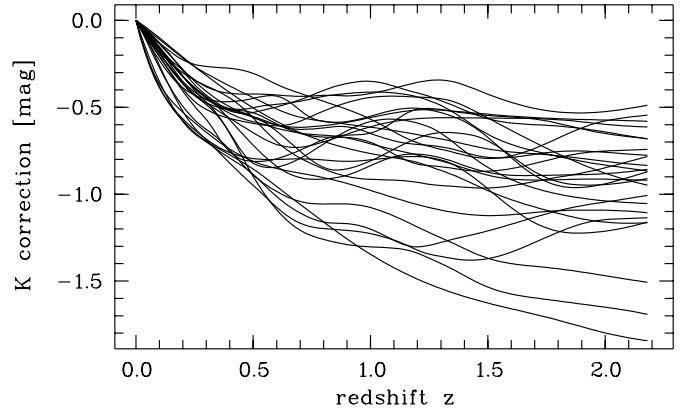


**Fig. 1.** Individual  $B$  band  $K$  corrections of the 25 sample QSOs, expressed in magnitudes as a function of redshift.

a more convex shape – in direct competition with the tendency of real quasar spectra to show a concave continuum energy distribution. The geometric mean, on the other hand, preserves the large-scale shape information much better and is therefore preferred.

Low- and high-redshift subsets were obtained by splitting the sample at  $z = 0.3$ , isolating 7 objects with luminosities much higher than the low-redshift QSOs. The mean  $K$  relations obtained from these two subsets are completely consistent with each other, revealing no discernible trends with luminosity and/or redshift. The same result was obtained after a splitting into radio-loud and radio-quiet subsets. Henceforth, only the average  $K(z)$  computed from the full sample is used. This is displayed in Fig. 2 together with a few comparison relations. Table 2 gives  $K(z)$  for the  $B$  band as a numerical array, sampled in redshift intervals of 0.1.

In addition to the mean  $K$  correction, it is important to have a realistic estimate of the *dispersion* around the mean. If this dispersion is large, the prediction of absolute magnitude involves an inherently stochastic component that is difficult to incorporate in luminosity function determinations (see discussion below). I have computed the standard deviation  $\sigma_K(z)$  around the mean  $K$  relation for the 25 quasars; this is shown by the solid line in Fig. 3. As the form of the distribution of  $K$  at given  $z$  around the average is not necessarily Gaussian, the standard deviation gives only an approximate idea of the true dispersion.

## 2.2. Emission lines

The data assembled so far describe only the continuum shape, systematically avoiding contamination by strong emission lines. However, broad-band photometric measurements of quasars usually contain a certain line contribution. This can be described by an emission line correction  $\Delta K_e(z)$ , to be added to the continuum  $K$  term. The correction is necessarily negative, and its magnitude is usually small, except for  $z > 2.2$  where  $\text{Ly}\alpha$  becomes important. I have computed a mean line correction using the emission lines strengths listed by Francis et al. (1991). Given the large number of contributing objects, these values

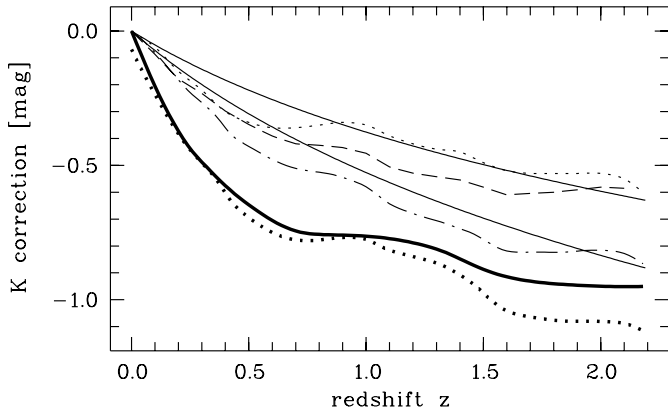


**Fig. 2.** Average  $K$  correction, for the continuum only (solid thick line), and for continuum plus lines as described in the text (dotted thick line). The empirical relations from Cristiani & Vio (1990) and Natali et al. (1998) are shown dotted and dashed, respectively, while the dot-dashed line shows the LBQS relation. The thin solid lines represent power-law relations for spectral indices  $\alpha = -0.5$  (upper) and  $\alpha = -0.3$  (lower).

**Table 2.** Numerical values of the derived  $B$  band  $K(z)$  correction for continuum, lines, and combined relation. A table with finer step size in  $z$ , as well as similar relations for other photometric bands are available in electronic form from the author.

$z$	$K_c$	$\Delta K_e$	$K_{\text{total}}$
0.0	0.00	-0.07	-0.07
0.1	-0.21	-0.03	-0.24
0.2	-0.37	-0.01	-0.38
0.3	-0.49	-0.00	-0.49
0.4	-0.58	-0.03	-0.60
0.5	-0.65	-0.05	-0.70
0.6	-0.71	-0.04	-0.75
0.7	-0.74	-0.03	-0.78
0.8	-0.76	-0.02	-0.78
0.9	-0.76	-0.01	-0.77
1.0	-0.76	-0.01	-0.78
1.1	-0.77	-0.04	-0.82
1.2	-0.79	-0.05	-0.84
1.3	-0.81	-0.05	-0.86
1.4	-0.85	-0.06	-0.91
1.5	-0.89	-0.09	-0.98
1.6	-0.92	-0.13	-1.04
1.7	-0.93	-0.13	-1.06
1.8	-0.94	-0.14	-1.08
1.9	-0.95	-0.13	-1.08
2.0	-0.95	-0.13	-1.08
2.1	-0.95	-0.14	-1.09
2.2	-0.96	-0.17	-1.14

are presumably quite representative for intermediate-luminosity quasars. The  $K$  correction values are listed in Table 2. Since  $H\beta$  and  $H\gamma$  are included, the resulting  $\Delta K_e(z)$  are  $< 0$  even at very low redshift. The ‘total’  $K$  correction is then the sum of line and continuum terms; this is shown by the dotted line in Fig. 2.

Any dispersion in line strengths acts effectively like an additional uncertainty of the mean correction. The measurements

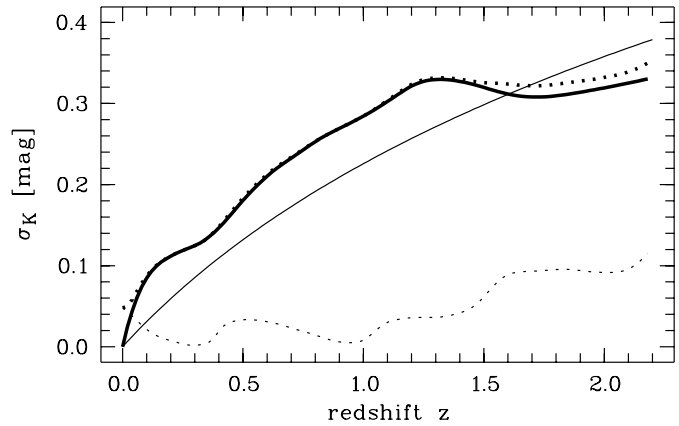


**Fig. 3.** Standard deviation ( $1\sigma$ ) of the individual  $K$  corrections for the sample QSOs around the mean (thick solid line). The thin solid line gives the expected scatter for power law spectra with a dispersion of  $\pm 0.3$  in spectral index  $\alpha$ . Thin dotted line: Uncertainty of emission line correction  $\Delta K_e(z)$ , estimated as described in the text; thick dotted line: Combined uncertainty of continuum plus line correction.

of Francis et al. (1991) indicate that the rms dispersion in equivalent widths is of the order of  $\sigma_{W_0} \approx 0.7 W_0$ . Assuming this spread for all lines, the resulting uncertainties for the mean line correction are shown by the dotted line in Fig. 3. It can be seen that while the line correction is a small but systematic effect, its contribution to the dispersion in  $K(z)$  is completely negligible. As a possible caveat one should keep in mind that the distribution of  $W_0$  values in quasar samples is far from being Gaussian, and very strong lines are much more common than for a normal distribution.

If spectra exist of the target quasars, even if of non-spectrophotometric quality, the line terms could be determined individually, and there would be no need for a *mean* line correction. Usually this should be possible for spectroscopically complete quasar samples. On the other hand, the uncertainties in the *continuum* totally dominate the  $K$  relation, so that a mean line correction is perfectly adequate as long as it is unbiased. This also enables an easier comparison of different quasar samples, not for all of which individual corrections may be available.

### 3. Discussion

Two important features of the newly determined  $K$  relation, called  $K_{\text{qed}}$  henceforth (after the ‘Atlas of quasar energy distributions’ upon which it is based), are apparent from Fig. 2: (1) The corrections are much larger (by absolute value) than in the ‘canonical’ relations. (2) The relation is poorly approximated by a single power-law. A sharp change of slope occurs around  $z \simeq 0.6$ , and separates a steep low-redshift from a flatter high-redshift part.

While a single value of  $\alpha$  is thus clearly not acceptable, it still may be possible to make local approximations within certain redshift intervals. Fig. 4 shows  $K_{\text{qed}}$  plotted against  $\log(1+z)$ ; power law relations appear here as straight lines. For  $z < 0.5$ , the function  $K[\log(1+z)]$  is almost perfectly linear, with an

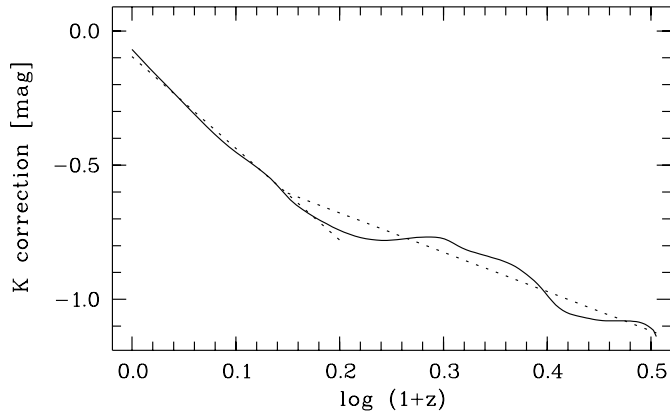


**Fig. 4.**  $K$  correction plotted against  $\log(1+z)$ . The dotted lines show the local power law approximations given in Table 3.

**Table 3.** Local power law approximation parameters for the  $K$  correction in some redshift intervals.

$z$ range	$\alpha$	$K(0)$	
0–0.3	+0.52	–0.08	
0–0.6	+0.36	–0.10	
0–0.6	+0.37	–0.07	(continuum only)
0.4–2.2	–0.45	–0.42	
0.4–2.2	–0.60	–0.48	(continuum only)

rms departure less than 0.01 mag. At higher  $z$ , there are more bends and wiggles, and the rms difference to a straight line is now 0.04 mag. Table 3 gives fit parameters for the usual power law formula:  $K(z) = K(0) - 2.5(1 + \alpha) \log(1 + z)$ , to be applied to low and high redshift regions separately. Note that the slope  $\alpha$  for the medium to high redshift regime is very close to the canonical value of  $-0.5$ ; however,  $K(z)$  is now offset by almost half a magnitude with respect to the  $z = 0$  reference.

The change of slope is also visible in the empirical relation of Cristiani & Vio (1990), but is much less pronounced there. Their  $K$  correction was based on a composite spectrum constructed from optical spectra of 47 QSOs at predominantly medium and high redshifts, hence each QSO spectrum contributed only to a small section of  $K(z)$ . Only very few low-redshift objects were in their sample, which may be not representative for small  $z$ .

Francis et al. (1991) constructed a composite spectrum based on more than 700 individual spectra from the ‘Large Bright Quasar Survey’ (LBQS, Hewett et al. 1995). A  $K(z)$  relation based on these data was presented by Hewett (1992) which is also shown in Fig. 2. The LBQS-based relation is much steeper than that of Cristiani & Vio (1990) and comes close to  $K_{\text{qed}}$  at higher redshifts, but is still inconsistent with it in the low-redshift regime.

Natali et al. (1998) recently determined  $K(z)$  by averaging over spectral indices defined over fixed wavelength intervals in the QSO rest frames, a procedure that avoids the bias to reduce the concave shape of single quasar spectra. The empirically determined  $\alpha(\lambda)$  by Natali et al. shows indeed a sharp turnover around  $3000 \text{ \AA}$ , corresponding to  $z \simeq 0.6$  for the  $B$  band. How-

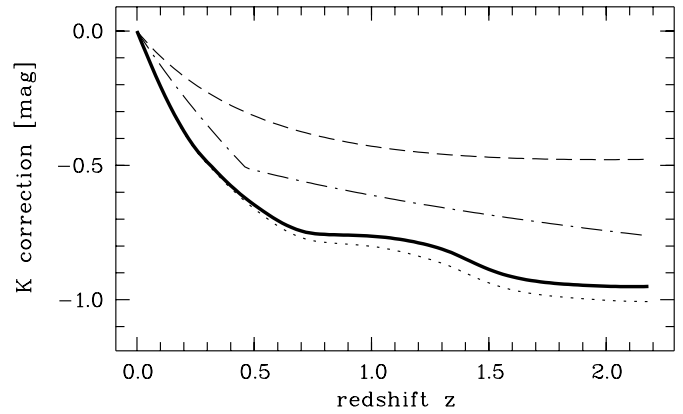


**Fig. 5.**  $K$  corrections determined by alternative methods, as discussed in the text.  $K_{\text{qed}}$  (continuum only) is shown by a thick line as in Fig. 2, the dotted line displays the result after taking the *arithmetic mean* of the spectra. The dashed line shows the reconstructed continuum  $K(z)$  from Natali et al. (1998), while the alternative two-power law relation mentioned in the text is plotted dot-dashed.

ever, this turnover is hardly discernible in their  $K(z)$  relation, which differs only insignificantly (by  $< 0.1$  mag) from the earlier Cristiani & Vio (1990) determination.

Comparing all available determinations of the  $K$  correction of quasars in Fig. 2, it seems that the largest discrepancies arise at low redshift where the departure from an overall power law fit is most prominent. At higher redshifts the different versions of  $K(z)$  appear to be more or less parallel and mainly shifted with respect to each other, and the magnitude of these shifts is determined by the slope at low redshift. The origin of this diversity is probably a mixed bag of several issues. First, the overall shape of the LBQS relation seems to be more similar to a power law than  $K_{\text{qed}}$ . This could be due to different sample properties, but it may also be influenced by the above mentioned tendency that averaged composite spectra look less concave than the individual input spectra. Note that this *cannot* explain the fact that  $K_{\text{qed}}$  is larger (by absolute value) than the other relations, as the effect goes the opposite way. This is illustrated in Fig. 5 where I show an alternative  $K_{\text{qed}}(z)$  relation based on the same input data, but computed from the arithmetic mean of the spectra. However, the effect is small in this case.

The analysis of Natali et al. (1998) warrants some reconsideration. They computed the  $K$  correction from a linear fit to their measurements of  $\alpha(\lambda)$ , and this fit produces a local spectral slope that is significantly shallower, in the low- $z$  regime, than the actual data indicate. A softer spectral slope implies a smaller absolute  $K$  correction, and this is propagated towards high redshift. To assess the strength of this effect, I have redetermined the  $K(z)$  relation from the data of Natali et al. (1998), but instead of a smooth linear function  $\alpha(\lambda)$  I have simply assumed a discontinuous transition of slope at  $\lambda = 3000 \text{ \AA}$  from  $\alpha = +0.23$  to  $\alpha = -0.7$ , which are their measured values left and right of the turnover. The resulting  $K$  correction (continuum only) is also shown in Fig. 5 (compared to the reconstructed continuum relation from Natali et al. 1998). This relation is much steeper at

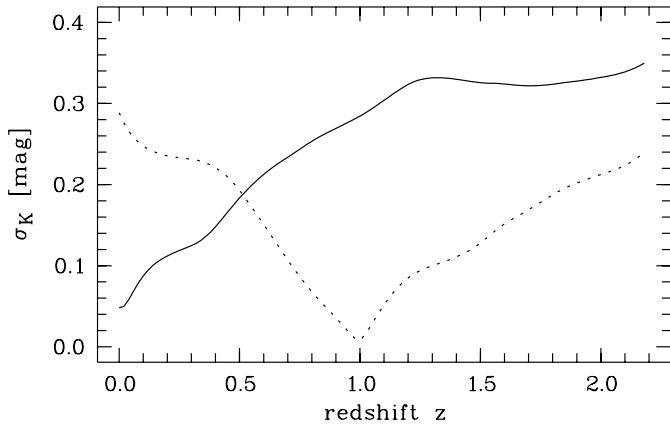


**Fig. 6.** Standard deviation ( $1\sigma$ ) of the individual  $K$  corrections taken for different reference wavelengths. The solid line is for  $\lambda_{\text{ref}} = 4400 \text{ \AA}$  or  $z_{\text{ref}} = 0$  (same as thick line in Fig. 3), while the dashed line is for  $\lambda_{\text{ref}} = 2200 \text{ \AA}$  ( $z_{\text{ref}} = 1$ ).

low  $z$  and actually not very different from the double power law fit to  $K_{\text{qed}}$  described above. I conclude that the spectral turnover in the data of Natali et al. is nearly as strong as it is for the Elvis et al. (1994) sample used here (cf. Table 3), and that the discrepancies between the Natali et al. results and those presented in this paper are mainly due to methodical differences.

## 4. Consequences for quasar evolution

### 4.1. Evolution rates

If the  $K$  correction derived above is representative for QSOs at all redshifts  $z < 2.2$ , the luminosities especially of high-redshift quasars are systematically lower than conventionally estimated. The discrepancy steeply increases between  $z = 0$  and  $z = 0.6$ , after which it remains more or less at the offset value of  $\sim 0.4$  magnitudes as derived above. Because of the steep slope of the bright end of the quasar luminosity function, the space densities of luminous QSOs are correspondingly smaller by a factor of  $\sim 3$ , significantly reducing the inferred strong evolution of the quasar population.

In the past ten years, quasar evolution has been most commonly parameterised as ‘pure luminosity evolution’ (PLE), promoted for optically selected QSOs particularly by Boyle et al. (1987, 1988). In this picture, the luminosity function is assumed to be logarithmically shape-invariant and shifted in cosmic time, along with characteristic QSO luminosities evolving as  $L(z) \propto (1+z)^{k_L}$ . The evolution parameter  $k_L$  is generally found to be  $k_L \simeq 3.2\text{--}3.5$ , for different input samples and based on a  $K$  correction similar to an  $\alpha = -0.5$  power law.<sup>1</sup>

Switching to a different  $K$  correction will necessarily change the value of the parameter  $k_L$ , by an amount directly

<sup>1</sup> It should be noted that there is now strong evidence that the PLE picture is overly simplified, and that it does not permit an adequate description of the evolution of the quasar population. This seems to hold for both optical (cf. Wisotzki 1999) and X-ray domains (Hasinger et al. 1999).

related to the change of average luminosities for high-redshift QSOs. The offset of  $+0.4$  mag derived above is immediately mirrored by a corresponding decrease of  $k_L$ , the exact amount of which depends on the details of the analysis.

As an example, Boyle et al. (1990) obtained  $k_L = 3.5$  from a maximum likelihood analysis of their faint UV excess sample, using  $\alpha = -0.5$ . A two-dimensional Kolmogoroff-Smirnoff test indicates a high degree of consistency between sample and model. Adopting one of the published empirical  $K$  corrections based on composite spectra changes in fact very little: The same parameter set, in particular the same  $k_L$ , is fully consistent with the data for both the relations of Cristiani & Vio (1990) and of Natali et al. (1998). Adopting, on the other hand, the  $K_{\text{qed}}$  relation derived in this paper, the model becomes highly inconsistent with the sample, and parameter modifications are required. Reducing  $k_L$  to a value of 3.0, leaving all other parameters unchanged, leads to full recovery of the model performance.

This reduction of inferred evolution by  $\Delta k_L = 0.6$  is interesting, as it might resolve a puzzling phenomenon: With the advent of deep X-ray surveys in the past few years, PLE models were also applied to samples of X-ray selected AGN and claimed to be an equally good description as in the optical domain (e.g., Boyle et al. 1993; Jones et al. 1997). However, the PLE parameter  $k_L$  was always found to be significantly smaller in X-ray samples, typically  $k_L \simeq 2.5\text{--}3$ . It appears now perfectly possible that the optical value was systematically overestimated due to incorrect  $K$  corrections used, and that the apparent discrepancies between the two domains must be considered – at least partly – as artefacts.

### 4.2. Ultraviolet vs. optical luminosities

Reducing quasar luminosities to rest-frame optical passbands introduces considerable uncertainty in the estimation of absolute magnitudes, especially for quasars at higher redshifts. As an alternative, it is possible to adopt another reference passband which is located *within* the sampled spectrophotometric range. The shape of QSO spectra and the  $K(z)$  correction can be consulted to guide this choice: Figs. 2 and 3 show that at  $z = 1.0$  the effects of the *little blue bump* are largely redshifted out of the  $B$  band, and that also the interference of emission lines is close to zero. In fact, one of the few reliable continuum points in the UV part of quasar spectra is at  $\lambda = 2200 \text{ \AA}$ , just the effective wavelength of the  $B$  band at  $z = 1$ . Notice also the proximity to the early suggestion by Schmidt (1968) to refer to  $\lambda = 2500 \text{ \AA}$  – however, that wavelength suffers from higher contamination by the ‘little blue bump’.

The corresponding relation  $K'(z)$  is readily obtained for the  $B$  band by shifting the mean  $K_{\text{qed}}(z)$  by an offset of  $-K(1) = 0.763$  mag (continuum value). It is interesting to investigate the resulting standard deviation  $\sigma_{K'}(z)$ : Per definition it vanishes at  $z = 1$  (apart from the emission line contribution), but it is also much smaller than  $\sigma_K$  at all but the lowest redshifts. Of course, this simply illustrates the fact that for a high-redshift QSO and using  $B$  band photometry, it is more accurate to estimate its monochromatic luminosity at  $\lambda = 2200 \text{ \AA}$  than at  $\lambda = 4400 \text{ \AA}$ .

As first pointed out by Giallongo & Vagnetti (1992), any allowed dispersion in the true  $K$  corrections for the quasars in a given sample reduces the amount of evolution inferred. This effect has been quantitatively studied in the Monte-Carlo simulations of La Franca & Cristiani (1997): A dispersion in spectral index of  $\sigma_\alpha = 0.3$  reduces the luminosity evolution index  $k_L$  by  $\sim 0.1$ , while  $\sigma_\alpha = 0.5$  already gives a three times larger reduction. Fig. 3 shows that  $\sigma_\alpha \simeq 0.3$  is a reasonable approximation for the dispersion  $\sigma_K$ , even though the spectra as such are not well described by power laws, implying that the Giallongo & Vagnetti effect will be small but noticeable. After a transformation to  $\lambda_{\text{ref}} = 2200 \text{ \AA}$  (or  $z = 1$ ) as reference, the standard deviation is  $\sigma_{K'} < 0.2$  nearly everywhere. In this case, the effect of spectral slope dispersion can be safely neglected, at least as far as the estimation of evolution parameters is concerned.

## 5. Conclusions

A good knowledge of quasar spectral energy distributions in the optical / ultraviolet domain is essential to estimate rest-frame luminosities of QSOs from single-channel photometry, such as is commonly used for studying the evolution of optically selected QSOs. If the quasar optical/UV SEDs analysed in this paper are representative for QSOs as a whole, the luminosities and space densities of high-redshift  $B$ -band selected quasars have hitherto been systematically overestimated. In that case, the evolution rates of optically selected QSOs have also to be corrected downwards, making them more similar to those of X-ray selected AGN.

It is still possible that the intrinsic SEDs of high-redshift quasars may be different from those at low  $z$ . However, there are good reasons to believe that this is not so. First, no systematic trends with luminosity or redshift are visible in the present sample (which admittedly does not reach very high redshifts). Second, the effective rest frame optical/UV continuum spectral indices of a sample of high- $z$  QSOs determined by Francis (1996) are consistent with the low-redshift data analysed here. Third, the spectral indices determined by Natali et al. (1998) agree very well with the properties of the sample analysed in this paper.

The  $K$  correction has been determined in this paper from 25 individual SEDs, each of which is available over the full relevant optical-UV wavelength range. The same procedure is, in principle, also applicable to high-redshift QSOs, using multi-band optical and near-infrared photometry. Besides the important task of assessing whether quasar SEDs evolve with  $z$ , such data would also permit the direct construction of appropriate high-redshift  $K$  corrections and the associated dispersions. Only then will it be possible to quantitatively determine the evolution rates of quasars over large redshift ranges.

## References

- Boyle B.J., Fong R., Shanks T., Peterson B.A., 1987, MNRAS 227, 717
- Boyle B.J., Shanks T., Peterson B.A., 1988, MNRAS 235, 935
- Boyle B.J., Fong R., Shanks T., Peterson B.A., 1990, MNRAS 243, 1
- Boyle B.J., Griffiths R.E., Shanks T., Stewart G.C., Georgantopoulos I., 1993, MNRAS 260, 54
- Cristiani S., Vio R., 1990, A&A 227, 385
- Elvis M., Wilkes B.J., McDowell J.C., et al., 1994, ApJS 95, 1
- Francis P.J., 1996, Publ. Astron. Soc. Austr. 13, 212
- Francis P.J., Hewett P.C., Foltz C.B., et al., 1991, ApJ 373, 465
- Giallongo E., Vagnetti F., 1992, ApJ 396, 411
- Hasinger G., Lehmann I., Giacconi R., et al., 1999, In: Highlights in X-ray astronomy. in press, astro-ph/9901103
- Hewett P.C., 1992, In: Duschl W.J., Wagner S.J. (eds.) Physics of Active Galactic Nuclei. Springer-Verlag, p. 649
- Hewett P.C., Foltz C.B., Chaffee F.C., 1995, AJ 109, 1498
- Jones L.R., McHardy I.M., Merryfield M.R., et al., 1997, MNRAS 285, 547
- Kolman M., Halpern J.P., Shrader C.R., et al., 1993, ApJ 402, 514
- La Franca F., Cristiani S., 1997, AJ 113, 1517
- Natali F., Giallongo E., Cristiani S., La Franca F., 1998, AJ 115, 397
- Richstone D.O., Schmidt M., 1980, ApJ 235, 361
- Schmidt M., 1968, ApJ 151, 393
- Schmidt M., Green R.F., 1983, ApJ 269, 352
- Wisotzki L., 1999, A&A, submitted
- Wisotzki L., Wamsteker W., Reimers D., 1991, A&A 247, 17